Calculated Isomeric Populations of Er@C_{82}

Zdeněk Slanina,[*,a,b] Filip Uhlík,[c] Shuaifeng Hu,[b] Takeshi Akasaka,[b] Xing Lu,[b] Ludwik Adamowicz[a]

[a] *Department of Chemistry and Biochemistry, University of Arizona, Tucson, AZ 85721-0041, USA*

[b] *State Key Laboratory of Materials Processing and Die & Mould Technology, School of Material Science and Engineering, Huazhong University of Science and Technology, Wuhan 430074, China*

[c] *Department of Physical and Macromolecular Chemistry, Charles University in Prague, Faculty of Science, Albertov 6, 128 43 Praha 2, Czech Republic*

Abstract

Relative populations of the four energy-lowest IPR (isolated-pentagon-rule) isomers of Er@C_{82} under the high-temperature synthetic conditions are computed using the Gibbs energy based on characteristics from the density functional theory calculations (B3LYP/6-31+G*∼SDD energetics, B3LYP/6-31G*∼SDD entropy). Two leading isomers are predicted - Er@$C_{2v}(9)$-C_{82} and Er@$C_s(6)$-C_{82}. The calculated equilibrium isomeric relative populations agree with available observations. As Er@C_{82} is one of the metallofullerenes recently used as dopants for improvement of efficiency and stability of perovskite solar cells, the calculations should help in finding rules for further selections of fullerene endohedrals for such new applications in photovoltaics.

---

*Corresponding author; E-mail: zdeneks@email.arizona.edu

Introduction

Recently, improved efficiency and stability of perovskite solar cells has been observed[1] after additions of a metallofullerene, namely Er@C_{82} (the improvements should partly be related to its hydrophobicity). Another metallofullerene, Dy@C_{82}, has also been studied[2,3] as a dopant for organic photovoltaics[4] in order to enhance quantum yields. Two isomers are known[5−8] for Er@C_{82}, they differ in their carbon cages C_{82} (this is also the case of Dy@C_{82} and other C_{82}-based endohedrals[9]), namely labeled Er@$C_{2v}(9)$-C_{82} and Er@$C_s(6)$-C_{82} (or Er@$C_s(c,6)$-C_{82}, also Er@C_s; 6-C_{82}). Actually, there are two labeling conventions[9] for the C_{82} IPR (isolated pentagon rule) cages considered in the literature. The older system deals with the symmetries of the carbon cages (in fact, the highest topological symmetries, regardless possible symmetry reductions - like by the Jahn-Teller distortions): $C_{3v}(a)$, $C_{3v}(b)$, C_{2v}, $C_2(a)$, $C_2(b)$, $C_2(c)$, $C_s(a)$, $C_s(b)$, and $C_s(c)$. The newer labeling system works with serial isomer-enumeration numbers, the assignment is: $C_{3v}(a)$; 7, $C_{3v}(b)$; 8, C_{2v}; 9, $C_2(a)$; 3, $C_2(b)$; 1, $C_2(c)$; 5, $C_s(a)$; 2, $C_s(b)$; 4, and $C_s(c)$; 6. Various metals can be encapsulated in the C_{82} cages, frequently producing at least two isomeric endohedrals.[9−16] In this report, the isomeric relative populations or stabilities are calculated in the set of four Er@C_{82} IPR isomers lowest in the potential energy. Such relative stability evaluations are needed in interpretation of observations and for selection and preparation of the particular species useful for applications.

Thermodynamic stabilities of nanocarbons, and in particular metallo-

fullerenes, are frequently calculated using just terms of potential energy. However, there are already several computational treatments[17−26] showing that the complete Gibbs energy should be employed instead - as the entropy part becomes increasingly important with increasing temperature. Consequently, in a set of isomers a species that is not the lowest in potential energy can nevertheless represent the most populated isomer at high synthetic temperatures (in particular used in nanocarbon syntheses). Other higher-energy structures can moreover exhibit relative-stability interchanges with increasing temperature. Obviously, it is not possible to predict such complex relative-stability behavior only from the potential energies. Hence, calculations are performed in this report on the equilibrium relative populations of four potential-energy lowest Er@C_{82} IPR isomers at elevated temperatures, considering both enthalpy and entropy component of the Gibbs energy in order to predict their equilibrium isomeric populations at synthetic conditions.

Calculations

The molecular-structure optimization of the Er@C_{82} isomers started with the molecular geometries optimized in a combined basis set - the standard 3-21G basis[27] for C atoms and SDD basis[28] with the SDD effective core potential on Er atom (denoted here as 3-21G∼SDD), employing density functional theory (DFT) approach. The DFT treatment uses here

Becke's three-parameter functional[29] combined with the non-local Lee-Yang-Parr correlation functional,[30] i.e., the unrestricted B3LYP/3-21G∼SDD approach. Moreover, the structures were further re-optimized using the standard 6-31G* basis set[31] for C atoms, i.e., the B3LYP/6-31G*∼SDD level. The calculations are carried out for the triplet electronic state as the multiplicity produces the lowest energy at the considered computational levels. The geometry optimizations are carried out with the analytical energy gradient. The geometry optimizations at the B3LYP/3-21G∼SDD and B3LYP/6-31G*∼SDD levels point out just three Er@C_{82} isomeric species sufficiently low in the potential energy (Table 1). All other isomers are at the B3LYP/6-31G*∼SDD level 9 or more kcal/mol higher than the lowest-energy isomer Er@C_{2v}(9)-C_{82} which (after combination with the entropy terms) would produce only insignificant relative populations. Moreover, the inter-isomeric separation energetics was further checked and refined with the B3LYP/6-31+G*∼SDD treatment (in the B3LYP/6-31G*∼SDD geometries). In the optimized B3LYP/6-31G*∼SDD geometries, the harmonic vibrational analysis was also performed with the analytical force-constant matrix in order to produce the vibrational spectra and especially the vibrational partition functions for the thermodynamic stability evaluations. The SCF wavefunction stability[32−34] was systematically tested throughout in order to avoid misleading unstable SCF solutions (that can appear quite frequently with nanocarbons). Moreover, in order to achieve the SCF convergency, various available[34] numerical options had to be applied. The computations

were carried out with the Gaussian 09 program package[34] on computers operating in parallel regime, mostly with 8-24 processors (with computational frequency up 3 GHz each and with the available operational memory up to 60 GB).

The relative equilibrium concentrations (considered in the terms of mole fractions x_i) in a set of m isomers can be expressed[35,36] with the help of their partition functions q_i and the enthalpies at the absolute zero temperature or ground-state energies $\Delta H^o_{0,i}$ (i.e., the relative potential energies enhanced by the vibrational zero-point energies) by a master formula:

$$x_i = \frac{q_i exp[-\Delta H^o_{0,i}/(RT)]}{\sum_{j=1}^{m} q_j exp[-\Delta H^o_{0,j}/(RT)]} \ , \qquad (1)$$

where R stands for the gas constant and T for the absolute temperature. Equation (1) is an exact formula that is derived[35] in statistical thermodynamics using the standard Gibbs energies of the isomers, supposing the conditions of the inter-isomeric thermodynamic equilibrium. Clearly enough, the reference energy level can be selected in such a way that one of the $\Delta H^o_{0,i}$ terms is equal to zero (the ground state energy of the lowest isomer is straightforwardly used[36] as the reference energy level). Rotational and vibrational partition functions are constructed[36] here employing the conventional rigid-rotator and harmonic-oscillator (RRHO) approximation. No frequency scaling is considered as it is not significant[37] for the x_i values at high temperatures. Finally, the chirality contribution[38] was included

accordingly (for an enantiomeric pair its partition function q_i is doubled). Although the temperature regions where fullerene or metallofullerene electric-arc syntheses take place is not well known, the recent observations[39] supply some arguments to expect it, for empty fullerenes, somewhere around 1300 K. Thus, the calculated results discussed here are also considered for the temperature region.

Actually, a modified[23,40] RRHO approach for description of the encapsulate motions is in fact considered here, following findings[41] that the encapsulated atoms can exhibit large amplitude vibrational motions, especially so at higher temperatures (if the motions are not restricted by cage derivatizations[42]). It can be expected that if the encapsulate is relatively free then, at sufficiently high temperatures, its motions in different cages will still yield about the same contribution to the partition functions. However, such similar contributions would then cancel out in Equation (1). This approximation is called[23,40] free, fluctuating, or floating encapsulate model (FEM) and needs two steps. In addition to suppression of the three lowest vibrational frequencies (representing the metal motions in the cage), the symmetries of the cages should be treated as the highest (topologically) possible, which reflects averaging effects of the large amplitude vibrational motions. For example, for the Er@C_{82} isomer based on the IPR $C_{2v}(9)$ cage (Table 1), the C_{2v} symmetry is considered within the FEM scheme though its static[43] symmetry (i.e., just after the geometry optimization) is only simple C_1 (Fig. 1). Generally speaking, the FEM treatment gives a better agreement[23,40] with the available

observed data compared to the conventional RRHO approach, and therefore the FEM approach is also applied here.

Results and Discussion

Table 1 reports the Er@C_{82} relative inter-isomeric energetics calculated at the two selected levels (namely, the differences in the potential energy without inclusion of the zero-point vibrational energies) for the four considered low-energy Er@C_{82} isomers with the IPR C_{82} cages[9,44] (the four possible IPR C_{82} symmetry types are thus included in the set). The lowest-energy Er@C_{82} isomer is the $C_{2v}(9)$ endohedral followed after about 2 kcal/mol by the $C_s(6)$ species (Fig. 1). Then, the $C_2(5)$ and $C_{3v}(8)$ endohedrals are located higher above the $C_{2v}(9)$ isomer by about 4 and 9 kcal/mol, respectively. It should be noted that the B3LYP/6-31G*∼SDD and B3LYP/6-31+G*∼SDD inter-isomeric separation energies are quite similar. The four isomers from Table 1 are considered in the following thermodynamic-stability treatment.

Table 2 presents selected calculated characteristics of the four potential-energy-lowest Er@C_{82} isomers. The B3LYP/6-31G*∼SDD calculated closest contacts r_{Er-C} between Er atom and the cages are around 2.5 Å and thus similar to the values found previously for other C_{82} based metallofullerenes.[9,15,44] The lowest vibrational frequencies ω_{low} given in Table 2 are in agreement with the supposed relatively-free motions of encapsulated metals in metallofullerenes. The B3LYP/3-21G∼SDD computed Mulliken atomic charges q_{Er} on Er are close to 2.2 (of the electron elementary charge).

The charge transfer to the cage is not distributed on the carbon atoms evenly, moreover, some carbons have negative but some positive Mulliken atomic charges (which is, by the way, of importance for repulsions between the cage carbons). In the case of the Er@C_{2v}(9)-C_{82} isomer the Mulliken atomic charge on the carbon atoms has values between -0.213 and +0.009. Similarly for the Er@C_s(6)-C_{82} isomer the Mulliken atomic charge varies from -0.219 to +0.012. Interestingly, the calculated total charge-transfer from the metals in the co-crystal[8] of Er@C_{2v}(9)-C_{82} with nickel-octaethylporphyrin is 3.1. The dipole moment calculated at the B3LYP/3-21G$\sim$SDD level has for the Er@C_{2v}(9)-C_{82} and Er@C_s(6)-C_{82} isomer value of 1.171 and 0.887 D, respectively. Let us mention for the completeness that the Mulliken charges from the 3-21G$\sim$SDD basis, in contrast to, e.g., the 6-31G*$\sim$SDD level, produce[25] for metallofullerenes a good agreement with the available observed charges.[45] Moreover, there are more general methodological reasons[46−49] why larger basis sets should not be used for the Mulliken charges - as they can sometimes produce rather unphysical values.[47]

Fig. 2 presents the key results of this study - temperature development of the relative equilibrium populations for the four potential-energy-lowest Er@C_{82} isomers in a wide temperature region. The relative populations are evaluated in the FEM treatment supplied with the B3LYP/6-31+G*$\sim$SDD energetics and B3LYP/6-31G*$\sim$SDD entropy. At very low temperatures the structure lowest in the $\Delta H^o_{0,i}$ scale must be dominant, i.e., the Er@C_{2v}(9)-C_{82} endohedral. However, the second potential-energy lowest species Er@C_s(6)-

C_{82} exhibits rather fast increase of its relative populations so that both isomers have comparable concentrations at high temperatures. On the other hand, the remaining two endohedrals, Er@$C_2(5)$ and Er@$C_{3v}(8)$-C_{82}, are rather negligible. At a temperature of 1300 K, the equilibrium populations are 40.9, 44.5, 13.4, and 1.2 % for the $C_{2v}(9)$, $C_s; 6$, $C_2; 5$, and $C_{3v}; 8$ isomers, respectively. Incidentally, in a stability evaluation without the entropic part (i.e., if only the simple Boltzmann factors[35,36] are considered) the relative isomeric populations at the same temperature of 1300 K are rather different: 59.3, 27.4, 11.5, and 1.7 % for the $C_{2v}(9)$, $C_s(6)$, $C_2(5)$, and $C_{3v}(8)$ isomers, respectively. The calculations agree with the available observations.[5−8] There are just two significantly produced Er@C_{82} isomers. The Er@$C_{2v}(9)$-C_{82} endohedral should be more populated of the two species. The temperature region for metallofullerene syntheses can be lower than that[39] (around 1300 K) for fullerenes (owing to catalytic effects by the metals involved). Interestingly, Er@$C_{2v}(9)$-C_{82} was recently used[1] as an additive for improving stability and performance of perovskite solar cells (the Er@$C_{2v}(9)$-C_{82} isomer is not prone[8] to dimerization in condensed phase - in contrast to Er@$C_s(6)$-C_{82}). Let us also add for the completeness that in contrast to the relative isomeric stabilities, the absolute stability of Er@C_{82} represents considerably more complex task as it requires not only its formation equilibrium constant but also the reaction partial pressures of carbon and Er vapor (virtually unknown from experiments).

There are some similarities with the results reported[11,23,50−54] in the

recent calculations of the C_{82} based metallofullerenes, exhibiting a comparable metal-to-cage charge transfer. Such similarities could be related to the structural feature that metallofullerenes are not formed by creation of a covalent bond but stabilized[55−59] by ionic bond instead. Let us also mention that observed isomeric populations can depend on employed metal form.[60] The issue could be related to the catalytic and kinetics aspects,[61−63] and thus to differing levels to which the expected inter-isomeric thermodynamic equilibrium could really be established in the synthesis. Yet another experimental issue is possible different solubility[64−66] of individual isomers in the solvents used for extractions. In future, the calculations should be checked at yet higher quantum-chemical levels, and the isomers in other spin states could be considered for a more comprehensive description of the system, too. Although the form of Equation (1) allows for some partial cancellation of higher contributions beyond the simple RRHO approximation like anharmonicity corrections,[67] further options for some improvements of the RRHO model should also be considered in future. Still, the present $Er@C_{82}$ results supply further evidence of applicability of the Gibbs-energy approach to the equilibrium populations of endohedral isomers, thus motivating related stability studies of even more complex species.[68−73]

Conclusions

The calculations of the relative equilibrium populations for the four potential-energy-lowest IPR isomers of $Er@C_{82}$ in the temperature region

used[39] in metallofullerene syntheses, employing the Gibbs energy (which is based on quantum-chemical molecular parameters), agree with available observed data. Further calculations are in progress in order to obtain a deeper, more detailed understanding of the functions of fullerene endohedrals as dopants for higher performance and stability of perovskite solar cells.[74−77] In addition to[1] Er@C_{82} also[2,3] Dy@C_{82} and[75−77] Gd@C_{82} are presently studied, especially their molecular and electronic structures as well as their energetics, thermodynamics, and also hydrophobicity.[78] The theoretical treatments should help to formulate molecular rules of rational selection of fullerene endohedrals for their applications in photovoltaics, first for the C_{82} based metallofullerenes and latter on even for other fullerene cages.

Acknowledgements

The reported research has been supported by the National Natural Science Foundation of China (21925104 and 92261204), the Hubei Provincial Natural Science Foundation of China (No. 2021CFA020), and the International Cooperation Key Project of Science and Technology Department of Shaanxi; and by the Charles University Centre of Advanced Materials/CUCAM (CZ.02.1.01/0.0/0.0/15 003/0000417), the MetaCentrum ((LM2010005) and CERIT-SC (CZ.1.05/3.2.00/08.0144) computing facilities. A very initial phase of the research line was supported by the Alexander von Humboldt-Stiftung and the Max-Planck-Institut für Chemie (Otto-Hahn-Institut), too.

References

1. Ye, X.; Yu, P.; Shen, W.; Hu, S.; Akasaka, T.; Lu, X. Er@C_{82} as a bifunctional additive to the spiro-OMeTAD hole transport layer for improving performance and stability of perovskite solar cells. Sol. RRL 2021, 5, 2100463.
2. Yang, S.; Fan, L.; Yang, S. Preparation, characterization, and photoelectrochemistry of LangmuirBlodgett films of the endohedral metallofullerene Dy@C_{82} mixed with metallophthalocyanines. J. Phys. Chem. B 2003, 107, 84038411.
3. Yang, S.; Fan, L.; Yang, S. LangmuirBlodgett films of poly(3-hexylthiophene) doped with the endohedral metallofullerene Dy@C_{82}: Preparation, characterization, and application in photoelectrochemical cells. J. Phys. Chem. B 2004, 108, 43944404.
4. Katz, E. A. Fullerene thin films as photovoltaic material, in Nanostructured Materials for Solar Energy Conversion, Soga, T., Ed., Elsevier, 2006, pp. 361-443.
5. Tagmatarchis, N.; Aslanis, E.; Shinohara, H.; Prassides, K. Isolation and spectroscopic study of a series of mono- and dierbium endohedral C_{82} and C_{84} metallofullerenes. J. Phys. Chem. B 2000, 104, 47, 1101011012.
6. Sanakis, Y.; Tagmatarchis, N.; Aslanis, E.; Ioannidis, N.; Petrouleas, V.; Shinohara, H.; Prassides, K. Dual-mode X-band EPR study of two isomers of the endohedral metallofullerene Er@C_{82}. J. Am. Chem. Soc. 2001, 123,

9924-9925.

7. Tagmatarchis, N.; Aslanis, E.; Prassides, K.; Shinohara, H. Mono-, di- and trierbium endohedral metallofullerenes: Production, separation, isolation, and spectroscopic study. Chem. Mater. 2001, 13, 23742379.

8. Hu, S.; Liu, T.; Shen, W.; Slanina, Z.; Akasaka, T.; Xie, Y.; Uhlik, F.; Huang, W.; Lu, X. Isolation and structural characterization of Er@C_{2v}(9)-$_{82}$ and Er@C_s(6)-$_{82}$: Regioselective dimerization of a pristine endohedral metallofullerene induced by cage symmetry. Inorg. Chem. 2019, 58, 2177-2182.

9. Slanina, Z.; Uhlík, F.; Feng, L.; Adamowicz, L. Calculated relative populations of Sm@C_{82} isomers. Fulleren. Nanotub. Carb. Nanostruct. 2018, 26, 233-238.

10. Slanina, Z.; Lee, S.-L.; Kobayashi, K.; Nagase, S. AM1 computed thermal effects within the nine isolated-pentagon-rule isomers of C_{82}. J. Mol. Struct. (THEOCHEM) 1995, 339, 89-93.

11. Nishibori, E.; Takata, M.; Sakata, M.; Inakuma, M.; Shinohara, H. Determination of the cage structure of Sc@C_{82} by synchrotron powder diffraction. Chem. Phys. Lett. 1998, 298, 79-84.

12. Slanina, Z.; Kobayashi, K.; Nagase, S. Ca@C_{82} isomers: Computed temperature dependency of relative concentrations. J. Chem. Phys. 2004, 120, 3397-3400.

13. Slanina, Z.; Kobayashi, K.; Nagase, S. Computed temperature development of the relative stabilities of La@C_{82} isomers. Chem. Phys. Lett.

2004, 388, 74-78.

14. Suzuki, M.; Slanina, Z.; Mizorogi, N.; Lu, X.; Nagase, S.; Olmstead, M. M.; Balch, A. L.; Akasaka, T. Single-crystal X-ray diffraction study of three Yb@C-82 isomers cocrystallized with Ni-II(octaethylporphyrin). J. Am. Chem. Soc. 2012, 134, 18772-18778.

15. Slanina, Z.; Uhlík, F.; Lee, S.-L.; Suzuki, M.; Lu, X.; Mizorogi, N.; Nagase, S.; Akasaka, T. Calculated temperature development of the relative stabilities of Yb@C_{82} isomers. Fulleren. Nanotub. Carb. Nanostruct. 2014, 22, 147-154.

16. Hu, Z.; Hao, Y.; Slanina, Z.; Gu, Z.; Shi, Z.; Uhlík, F.; Zhao, Y.; Feng, L. Popular C_{82} fullerene cage encapsulating a divalent metal ion Sm^{2+}: Structure and electrochemistry. Inorg. Chem. 2015, 54, 2103-2108.

17. Slanina, Z.; Lee, S.-L.; Adamowicz, L. C_{80}, C_{86}, C_{88}: Semiempirical and ab initio SCF calculations. Int. J. Quantum. Chem. 1997, 63, 529-535.

18. Slanina, Z.; Uhlík, F. Temperature dependence of the Gibbs energy ordering of isomers of Cl_2O_2. J. Phys. Chem. 1991, 95, 5432-5434.

19. Slanina, Z.; Zhao, X.; Lee, S.-L.; Ōsawa, E. C_{90} - Temperature effects on relative stabilities of the IPR isomers. Chem. Phys. 1997, 219, 193-200.

20. Uhlík, F.; Slanina, Z.; Ōsawa, E. C_{78} IPR fullerenes: Computed B3LYP/6-31G*//HF/3-21G temperature-dependent relative concentrations. Eur. Phys. J. D 2001, 16, 349-352.

21. Slanina, Z.; Zhao, X.; Uhlík, F.; Lee, S.-L.; Adamowicz, L. Computing enthalpy-entropy interplay for isomeric fullerenes. Int. J. Quantum Chem.

2004, 99, 640-653.

22. Slanina, Z.; Lee, S.-L.; Adamowicz, L.; Uhlík, F.; Nagase, S. Computed structure and energetics of La@C_{60}. Int. J. Quantum Chem. 2005, 104, 272-277.

23. Slanina, Z.; Lee, S.-L.; Uhlík, F.; Adamowicz, L.; Nagase, S. Computing relative stabilities of metallofullerenes by Gibbs energy treatments. Theor. Chem. Acc. 2007, 117, 315-322.

24. Wang, Y.; Morales-Martínez, R.; Zhang, X.; Yang, W.; Wang, Y.; Rodríguez-Fortea, A.; Poblet, J. M.; Feng, L.; Wang, S.; Chen, N. Unique four-electron metal-to-cage charge transfer of Th to a C_{82} fullerene cage: Complete structural characterization of Th@C_{3v}(8)-C_{82}. J. Am. Chem. Soc. 2017, 139, 5110-5116.

25. Slanina, Z.; Uhlík, F.; Nagase, S.; Akasaka, T.; Adamowicz, L.; Lu, X. Eu@C_{72}: Computed comparable populations of two non-IPR isomers. Molecules 2017, 22, 1053-1–1053-8.

26. Zhao, Y.; Li, M.; Zhao, R.; Zhao, P.; Yuan, K.; Li, Q.; Zhao, X. Unmasking the optimal isomers of Ti_2C_{84}: Ti_2C_2@C_{82} Instead of Ti_2C_{84}. J. Phys. Chem. C 2018, 122, 1314813155.

27. Binkley, J. S.; Pople, J. A.; Hehre, W. J. Self-consistent molecular orbital methods. 21. Small split-valence basis sets for first-row elements. J. Am. Chem. Soc. 1980, 102, 939-947.

28. Cao, X. Y.; Dolg, M. Segmented contraction scheme for small-core lanthanide pseudopotential basis sets. J. Mol. Struct. (Theochem) 2002,

581, 139-147.

29. Becke, A. D. Density-functional thermochemistry. III. The role of exact exchange. J. Chem. Phys. 1993, 98, 5648-5652.

30. Lee, C.; Yang, W.; Parr, R. G., Development of the Colle-Salvetti correlation-energy formula into a functional of the electron density. Phys. Rev. B 1988, 37, 785-789.

31. Hehre, W. J.; Ditchfield, R.; Pople, J. A. Self-consistent molecular orbital methods. 12. Further extensions of Gaussian-type basis sets for use in molecular-orbital studies of organic-molecules. J. Chem. Phys. 1972, 56, 2257-2261.

32. Schlegel, H. B.; McDouall, J. J. W. Do you have SCF stability and convergence problems? In Computational Advances in Organic Chemistry; Ögretir, C.; Csizmadia, I. G., Kluwer: Dordrecht, 1991, pp. 167-185.

33. Slanina, Z.; Uhlík, F.; Adamowicz, L. Computations of model narrow nanotubes closed by fragments of smaller fullerenes and quasi-fullerenes. J. Mol. Graph. Mod. 2003, 21, 517-522.

34. Frisch, M. J.; Trucks, G. W.; Schlegel, H. B.; Scuseria, G. E.; Robb, M. A.; Cheeseman, J. R.; Scalmani, G.; Barone, V.; Mennucci, B.; Petersson, G. A.; Nakatsuji, H.; Caricato, M.; Li, X.; Hratchian, H. P.; Izmaylov, A. F.; Bloino, J.; Zheng, G.; Sonnenberg, J. L.; Hada, M.; Ehara, M.; Toyota, K.; Fukuda, R.; Hasegawa, J.; Ishida, M.; Nakajima, T.; Honda, Y.; Kitao, O.; Nakai, H.; Vreven, T.; Montgomery, Jr.; J. A.; Peralta,

J. E.; Ogliaro, F.; Bearpark, M.; Heyd, J. J.; Brothers, E.; Kudin, K. N.; Staroverov, V. N.; Kobayashi, R.; Normand, J.; Raghavachari, K.; Rendell, A.; Burant, J. C.; Iyengar, S. S.; Tomasi, J.; Cossi, M.; Rega, N.; Millam, N. J.; Klene, M.; Knox, J. E.; Cross, J. B.; Bakken, V.; Adamo, C.; Jaramillo, J.; Gomperts, R.; Stratmann, R. E.; Yazyev, O.; Austin, A. J.; Cammi, R.; Pomelli, C.; Ochterski, J. W.; Martin, R. L.; Morokuma, K.; Zakrzewski, V. G.; Voth, G. A.; Salvador, P.; Dannenberg, J. J.; Dapprich, S.; Daniels, A. D.; Farkas, O.; Foresman, J. B.; Ortiz, J. V.; Cioslowski, J.; Fox, D. J. 2013. Gaussian 09, Rev. C.01, Wallingford, CT, Gaussian Inc.

35. Slanina, Z. Equilibrium isomeric mixtures: Potential energy hypersurfaces as originators of the description of the overall thermodynamics and kinetics. Int. Rev. Phys. Chem. 1987, 6, 251-267.

36. Slanina, Z. A Program for determination of composition and thermodynamics of the ideal gas-phase equilibrium isomeric mixtures. Comput. Chem. 1989, 13, 305-311.

37. Slanina, Z.; Uhlík, F.; Zerner, M. C. $C_5H_3^+$ isomeric structures: Relative stabilities at high temperatures. Rev. Roum. Chim. 1991, 36, 965-974.

38. Slanina, Z.; Adamowicz, L. On relative stabilities of dodecahedron-shaped and bowl-shaped structures of C_{20}. Thermochim. Acta 1992, 205, 299-306.

39. Cross, R. J.; Saunders, M. Transmutation of fullerenes. J. Am. Chem. Soc. 2005, 127, 3044-3047.

40. Slanina, Z.; Adamowicz, L.; Kobayashi, K.; Nagase, S. Gibbs energy-based treatment of metallofullerenes: Ca@C_{72}, Ca@C_{74}, Ca@C_{82}, and La@C_{82}. Mol. Simul. 2005, 31, 71-77.

41. Akasaka, T.; Nagase, S; Kobayashi, K.; Walchli, M.; Yamamoto, K.; Funasaka, H.; Kako, M.; Hoshino, T.; Erata, T. ^{13}C and ^{139}La NMR studies of La_2@C_{80}: First evidence for circular motion of metal atoms in endohedral dimetallofullerenes. Angew. Chem. Int. Ed. 1997, 36, 1643-1645.

42. Kobayashi, K.; Nagase, S.; Maeda, Y.; Wakahara, T.; Akasaka, T. La_2@C_{80}: Is the circular motion of two La atoms controllable by exohedral addition? Chem. Phys. Lett. 2003, 374, 562-566.

43. Slanina, Z. Contemporary Theory of Chemical Isomerism. Academia and D. Reidel Publ. Comp., Prague and Dordrecht, 1986, pp. 21-23.

44. Slanina, Z.; Uhlík, F.; Bao, L.; Akasaka, T.; Lu, X.; Adamowicz, L. Calculated relative populations for the Eu@C_{82} isomers. Chem. Phys. Lett. 2019, 726, 29-33.

45. Takata, M.; Nishibori, E.; Sakata, M.; Shinohara, H. Charge density level structures of endohedral metallofullerenes determined by synchrotron radiation powder method. New Diam. Front. Carb. Technol. 2002, 12, 271-286.

46. Hehre, W. J. A Guide to Molecular Mechanics and Quantum Chemical Calculations. Wavefunction, Irvine, 2003, p.435.

47. Jensen, F. Introduction to Computational Chemistry. Wiley, Chichester,

2017, p.319.

48. Campanera, J. M.; Bo, C.; Poblet, J. M. General rule for the stabilization of fullerene cages encapsulating trimetallic nitride templates. Angew. Chem. Int. Ed. 2005, 44, 7230-7233.

49. Slanina, Z.; Uhlík, F.; Pan, C.; Akasaka, T.; Lu, X.; Adamowicz, L. Computed stabilization for a giant fullerene endohedral: Y_2C_2@C_1(1660)-C_{108}. Chem. Phys. Lett. 2018, 710, 147-149.

50. Slanina, Z.; Uhlík, F.; Lee, S.-L.; Nagase, S. Structural and bonding features of Z@C_{82} (Z = Al, Sc, Y, La) endohedrals. J. Comput. Meth. Sci. Engn. 2010, 10, 569-574.

51. Slanina, Z.; Uhlík, F.; Shen, W.; Akasaka, T.; Lu, X.; Adamowicz, L. Calculations of the relative populations of Lu@C_{82} isomers. Fulleren. Nanotub. Carb. Nanostruct. 2019, 27, 710-714.

52. Slanina, Z.; Uhlík, F.; Akasaka, T.; Lu, X.; Adamowicz, L. Calculated relative thermodynamic stabilities of the Gd@C_{82} isomers. ECS J. Solid State Sci. Technol. 2021, 10, 071013-1–071013-4.

53. Meng, Q. Y.; Morales-Martínez, R.; Zhuang, J. X.; Yao, Y. R.; Wang, Y. F.; Feng, L.; Poblet, J. M.; Rodríguez-Fortea, A.; Chen, N. Synthesis and characterization of two isomers of Th@C_{82}: Th@C2v(9)-C_{82} and Th@C_2(5)-C_{82}. Inorg. Chem. 2021, 60, 11496-11502.

54. Slanina, Z.; Uhlík, F.; Feng, L.; Adamowicz L. Ho@C_{82} metallofullerene: Calculated isomeric composition. ECS J. Solid State Sci. Technol. 2022, 11, 053018-1–053018-4.

55. Andreoni, W.; Curioni, A. Freedom and constraints of a metal atom encapsulated in fullerene cages. Phys. Rev. Lett. 1996, 77, 834-837.

56. Popov, A. A.; Dunsch, L. Bonding in endohedral metallofullerenes as studied by quantum theory of atoms in molecules. Chem. Eur. J. 2009, 15, 9707-9729.

57. Slanina, Z.; Uhlík, F.; Lee, S.-L.; Adamowicz, L.; Akasaka, T.; Nagase, S. Computed stabilities in metallofullerene series: Al@C_{82}, Sc@C_{82}, Y@C_{82}, and La@C_{82}. Int. J. Quant. Chem. 2011, 111, 2712-2718.

58. Rodríguez-Fortea, A.; Balch, A. L.; Poblet, J. M. Endohedral metallofullerenes: A unique host-guest association. Chem. Soc. Rev. 2011, 40, 3551-3563.

59. Popov, A. A.; Yang, S.; Dunsch, L. Endohedral fullerenes. Chem. Rev. 2013, 113, 59896113.

60. Yang, H.; Yu, M.; Jin, H.; Liu, Z.; Yao, M.; Liu, B.; Olmstead, M. M.; Balch, A. L. Isolation of three isomers of Sm@C_{84} and X-ray crystallographic characterization of Sm@D_{3d}(19)-$_{84}$ and Sm@C_2(13)-C_{84}. J. Am. Chem. Soc. 2012, 134, 5331

61. Slanina, Z.; Zhao, X.; Uhlík, F.; Ozawa, M.; Ōsawa, E. Computational modelling of the metal and other elemental catalysis in the Stone-Wales fullerene rearrangements. J. Organomet. Chem. 2000, 599, 57-61.

62. Hao, Y.; Feng, L.; Xu, W.; Gu, Z.; Hu, Z.; Shi, Z.; Slanina, Z.; Uhlík, F. Sm@C_{2v}(19138)-C_{76}: A Non-IPR Cage Stabilized by a Divalent Metal Ion. Inorg. Chem. 2015, 54, 4243-4248.

63. Hao, Y.; Tang, Q.; Li, X.; Zhang, M.; Wan, Y.; Feng, L.; Chen, N.; Slanina, Z.; Adamowicz, L.; Uhlík, F. Isomeric $Sc_2O@C_{78}$ related by a single-step StoneWales transformation: Key links in an unprecedented fullerene formation pathway. Inorg. Chem. 2016, 55, 1135411361.

64. Jehlička, J.; Svatoš, A.; Frank, O.; Uhlík, F. Evidence for fullerenes in solid bitumen from pillow lavas of proterozoic age from Mítov (Bohemian Massif, Czech Republic). Geochem. Cosmochem. Acta, 67, 1495-1506 (2003)

65. Lian, Y.; Shi, Z.; Zhou, X.; Gu, Z. Different extraction behaviors between divalent and trivalent endohedral metallofullerenes. Chem. Mater. 2004, 16, 1704-1714.

66. Maeda, Y.; Tsuchiya, T.; Kikuchi, T.; Nikawa, H.; Yang, T.; Zhao, X.; Slanina, Z.; Suzuki, M.; Yamada, M.; Lian, Y.; Nagase, S.; Lu, X.; Akasaka, T. Effective derivatization and extraction of insoluble missing lanthanum metallofullerenes $La@C_{2n}$ (n=36-38) with iodobenzene. Carbon 2016, 98, 67-73.

67. Slanina, Z.; Uhlík, F.; Lee, S.-L.; Adamowicz, L.; Nagase, S. Computations of endohedral fullerenes: The Gibbs energy treatment. J. Comput. Meth. Sci. Engn. 2006, 6, 243-250.

68. Gueorguiev, G. K.; Stafström, S.; Hultman L. Nano-wire formation by self-assembly of silicon-metal cage-like molecules. Chem. Phys. Lett. 2008, 458, 170-174.

69. An, D.-Y.; Su, J.-G.; Li, C.-H.; Li, J.-Y. Computational studies on

the interactions of nanomaterials with proteins and their impacts. Chin. Phys. B, 2015, 24, 120504-1 – 120504-8.

70. Basiuk, V. A.; Tahuilan-Anguiano, D. E. Complexation of free-base and 3d transition metal(II) phthalocyanines with endohedral fullerene $Sc_3N@C_{80}$. Chem. Phys. Lett. 2019, 722, 146-152.

71. Tahuilan-Anguiano, D. E.; Basiuk, V. A. Complexation of free-base and 3d transition metal(II) phthalocyanines with endohedral fullerenes $H@C_{60}$, $H_2@C_{60}$ and $He@C_{60}$: The effect of encapsulated species. Diam. Rel. Mat. 2021, 118, 108510-1 – 108510-5.

72. Li, M.; Zhao, R.; Dang, J.; Zhao, X. Theoretical study on the stabilities, electronic structures, and reaction and formation mechanisms of fullerenes and endohedral metallofullerenes. Coor. Chem. Rev. 2022, 471, 214762-1 – 214762-12.

73. Slanina, Z.; Uhlík, F.; Adamowicz, L. Theoretical predictions of fullerene stabilities. In: Lu, X.; Akasaka, T.; Slanina, Z., Eds., Handbook of Fullerene Science and Technology, Springer, Singapore, 2022, p. 111-179.

74. Fang, Y.; Bi, C.; Wang, D.; Huang, J. The functions of fullerenes in hybrid perovskite solar cells. ACS Energy Lett. 2017, 2, 782794.

75. Okazaki, T.; Shimada, T.; Suenaga, K.; Ohno, Y.; Mizutani, T.; Lee, J.; Kuk, Y.; Shinohara H. Electronic properties of $Gd@C_{82}$ metallofullerene peapods: $(Gd@C_{82})_n$@SWNTs Appl. Phys. A 2003, 76, 475478.

76. Zhang, K. K.; Wang, C.; Zhang, M. H.; Bai, Z. B.; Xie, F. F.; Tan, Y. Z.; Guo, Y. L.; Hu, K. J.; Cao, L.; Zhang, S.; Tu, X. C.; Pan, D. F.; Kang,

L.; Chen, J.; Wu, P. H.; Wang, X. F.; Wang, J. L.; Liu, J. M.; Song, Y.; Wang, G. H.; Song, F. Q.; Ji, W.; Xie, S. Y.; Shi, S. F.; Reed, M. A.; Wang, B. G. A Gd@C_{82} single-molecule electret. Nature Nanotech. 2020, 15, 1019-1024.

77. Wu, B.-S.; An, M.-W.; Chen, J.-M.; Xing, Z.; Chen, Z.-C.; Deng, L.-L.; Tian, H.-R.; Yun, D.-Q.; Xie, S.-Y.; Zheng, L.-S. Radiation-processed perovskite solar cells with fullerene-enhanced performance and stability. Cell Rep. Phys. Sci. 2021, 2, 100646-1 – 100646-16.

78. Bologna, F.; Mattioli, E. J.; Bottoni, A.; Zerbetto, F.; Calvaresi, M. Interactions between endohedral metallofullerenes and proteins: The Gd@C_{60}lysozyme model. ACS Omega 2018, 3, 1378213789.

Table 1. Er@C_{82} relative potential energies $\Delta E_{pot,rel}$ for the IPR isomers calculated in the B3LYP/6-31G*∼SDD optimized structures

Species	$\Delta E_{pot,rel}$ / kcal.mol^{-1}	
	B3LYP/6-31G*∼SDD	B3LYP/6-31+G*∼SDD
$C_s(2)$	24.6	24.1
$C_2(1)$	19.8	19.1
$C_2(3)$	18.1	17.6
$C_s(4)$	15.2	14.9
$C_{3v}(7)$	9.76	9.54
$C_{3v}(8)$	9.14	9.10
$C_2(5)$	4.45	4.25
$C_s(6)^a$	2.03	1.99
$C_{2v}(9)^a$	0.0	0.0

[a]See Fig. 1.

Table 2. The selected characteristics of the four energy-lowest Er@C_{82} isomers - the closest Er-C contact[a] r_{Pr-C}, the Mulliken charge[b] on Er q_{Er}, the lowest vibrational frequency[a] ω_{low}

Species	r_{Er-C} / Å	q_{Er}	ω_{low} / cm^{-1}
$C_{3v}(8)$	2.342	2.335	5.6
$C_2(5)$	2.541	2.181	11.9
$C_s(6)^c$	2.430	2.198	14.5
$C_{2v}(9)^c$	2.457	2.211	20.0

[a]B3LYP/6-31G*∼SDD terms.

[b]B3LYP/3-21G∼SDD terms.

[c]See Fig. 1.

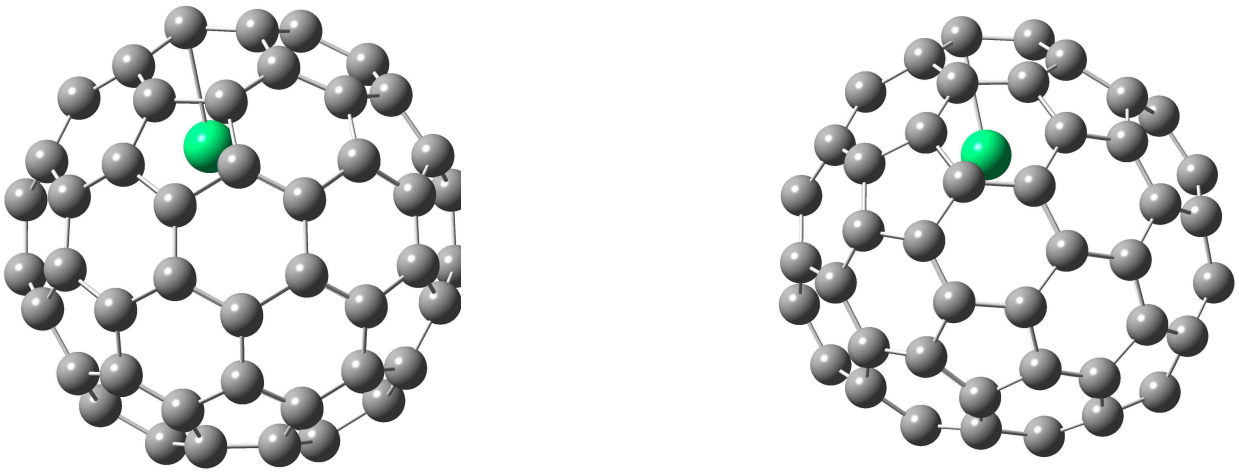

Fig. 1. The B3LYP/6-31G*∼SDD optimized structures of the two most populated Er@C_{82} isomers, Er@$C_{2v}(9)$-C_{82} left, Er@$C_s(6)$-C_{82} right (the shortest Er-C contact is indicated by a link).

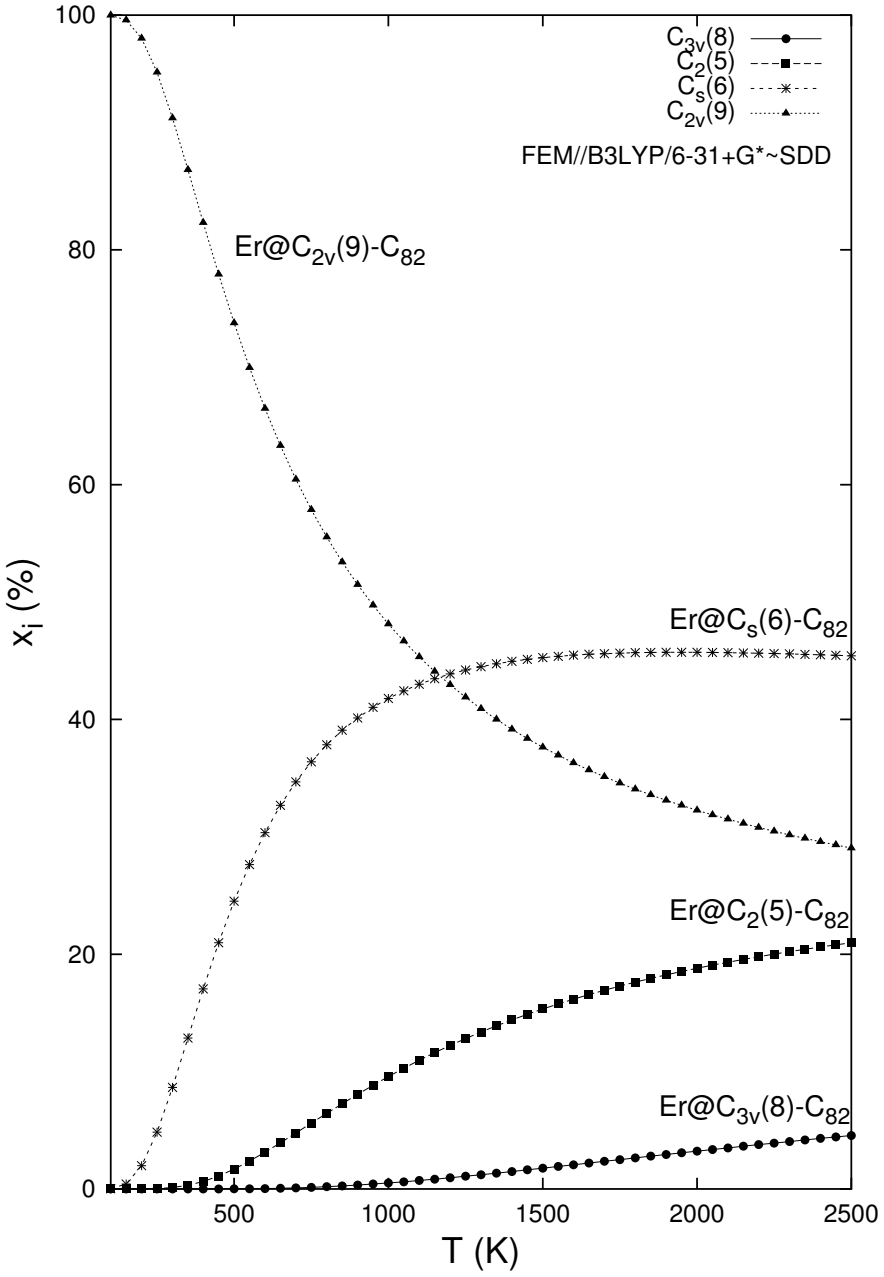

Fig. 2. The equilibrium relative populations of the Er@C_{82} isomers based on the FEM treatment with the B3LYP/6-31+G*∼SDD energetics and B3LYP/6-31G*∼SDD entropy.